

AD-A108 211

SCIENCE APPLICATIONS INC MCLEAN VA

F/6 20/4

SPECTRAL MODEL PREDICTIONS OF MEAN-SQUARE-SHEAR DISTORTION RATE--ETC(U)

N00014-81-C-0084

MAY 81 W GRABOWSKI, F C NEWMAN

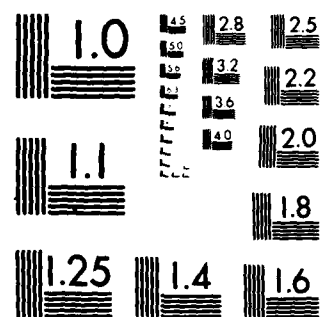
NL

UNCLASSIFIED

SAI-82-485-WA

1-1  
100-1

END  
DATE FILMED  
-182  
RTIC



MICROCOPY RESOLUTION TEST CHART  
NATIONAL BUREAU OF STANDARDS 1963-A

1  
Approved  
and calculated  
by [redacted]

SPECTRAL MODEL PREDICTIONS OF  
MEAN-SQUARE-SHEAR DISTORTION RATES

SAI-82-485-WA

RC  
RECEIVED  
1982  
FEB 22  
FBI - ATLANTA



ATLANTA • ANN ARBOR • BOSTON • CHICAGO • CLEVELAND • DENVER • HUNTSVILLE • LA JOLLA  
LITTLE ROCK • LOS ANGELES • SAN FRANCISCO • SANTA BARBARA • TUCSON • WASHINGTON

This document has been approved  
for public release and sale; its  
distribution is unlimited

SPECTRAL MODEL PREDICTIONS OF  
MEAN-SQUARE-SHEAR DISTORTION RATES

SAI-82-485-WA

OP TN 81-201-01

7 May 1981

Walt Grabowski  
Fred C. Newman  
Ocean Physics Division

for:  
Ocean Measurements Program  
Naval Ocean Research and Development Activity  
Bay St. Louis, Mississippi 39529

Contracts N00014-81-C-0084  
and N00014-81-C-0075

Accession For	
THIS GRA&I	<input checked="" type="checkbox"/>
STIC TAB	<input type="checkbox"/>
Unannounced	<input type="checkbox"/>
Distribution	<input type="checkbox"/>
<i>Little Bay</i>	
P.	
Distribution	
Availability Codes	
Avail and/or	
Other Special	
<i>A</i>	

SCIENCE APPLICATIONS, INC.  
P.O. Box 1303  
1710 Goodridge Drive  
McLean, Virginia 22102  
(703) 821-4300

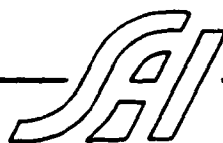
*SAI*

SECURITY CLASSIFICATION OF THIS PAGE (When Data Entered)

REPORT DOCUMENTATION PAGE		READ DIRECTIONS BEFORE COMPLETING FORM
1. REPORT NUMBER SAI-82-485-WA	2. GOVT ACCESSION NO. AD-A208 512	3. RECIPIENT'S CATALOG NUMBER
4. TITLE (and Subtitle) Spectral Model Predictions of Mean-Square-Shear Distortion Rates	5. TYPE OF REPORT & PERIOD COVERED TECHNICAL 20 Nov 80 - 7 May 81	
7. AUTHOR(s) Walt Grabowski Fred Newman	6. PERFORMING ORGS. REPORT NUMBER SAI-82-485-WA	
8. PERFORMING ORGANIZATION NAME AND ADDRESS Science Applications, Inc. 1710 Goodridge Drive McLean, Virginia 22102	9. PROGRAM ELEMENT, PROJECT, TASK AREA & WORK UNIT NUMBERS	
11. CONTROLLING OFFICE NAME AND ADDRESS	12. REPORT DATE 7 May 1981	
	13. NUMBER OF PAGES	
14. MONITORING AGENCY NAME & ADDRESS (if different from Controlling Office)	15. SECURITY CLASS. (of this report) UNCLASSIFIED	
	15a. DECLASSIFICATION/DOWNGRADING SCHEDULE N/A	
16. DISTRIBUTION STATEMENT (of this Report)  <i>[Redacted]</i>		
17. DISTRIBUTION STATEMENT (of the abstract entered in Block 20, if different from Report)		
18. SUPPLEMENTARY NOTES		
19. KEY WORDS (Continue on reverse side if necessary and identify by block number) Shear, wake distortion		
20. ABSTRACT (Continue on reverse side if necessary and identify by block number) It is possible to use a simple shear spectral model to produce some estimates of the mean-square velocity difference over given values of $\Delta z$ . The distortion of a fluid region (a wake cross section, say) of dimension L is clearly due to velocity differences over $\Delta z$ equal to L and smaller. In this note we explore the behavior of velocity differences over $\Delta z$ with a simple model for the shear spectral density function.		

TABLE OF CONTENTS

<u>Section</u>	<u>Page</u>
1      INTRODUCTION . . . . .	1
2      FORMULATION . . . . .	1
3      RESULTS . . . . .	5
4      DISCUSSION . . . . .	7
REFERENCES . . . . .	R-1



## 1.0 INTRODUCTION

It is possible to use a simple shear spectral model to produce some estimates of the mean-square velocity difference over given values of  $\Delta z$ . The distortion of a fluid region (a wake cross section, say) of dimension L is clearly due to velocity differences over  $\Delta z$  equal to L and smaller. In this note we explore the behavior of velocity differences over  $\Delta z$  with a simple model for the shear spectral density function.

## 2.0 FORMULATION

We represent the horizontal velocity field as a Fourier integral

$$\underline{U}(z) = \int_{-\infty}^{\infty} d\beta \underline{U}(\beta) e^{i\beta z} \quad (1)$$

where  $\underline{U}$  is the horizontal velocity vector,  $\underline{U}(\beta)$  is the Fourier component amplitude (complex) vector ( $U(\beta)$ ,  $V(\beta)$ ), and  $\beta$  is the vertical wavenumber. It is straightforward to show that

$$\begin{aligned} \langle |\underline{U}(z+\Delta z) - \underline{U}(z)|^2 \rangle &= \int_{-\infty}^{\infty} d\beta 4 \langle U(\beta) U^*(\beta) \rangle \\ &\times (1 - \cos \beta \Delta z) \end{aligned} \quad (2)$$

where the braces indicate ensemble averaging.

From (1) it is apparent that

$$E(\beta) = 2 \langle U(\beta) U^*(\beta) \rangle \quad (3)$$

is the horizontal kinetic energy wavenumber spectral density function (defined over positive  $\beta$ ). Using a trigonometric half-angle formula we can write (2) as

$$\langle |U(z+\Delta z) - U(z)|^2 \rangle = 4 \int_0^\infty d\beta E(\beta) \sin^2(\frac{1}{2}\beta \Delta z) \quad . \quad (4)$$

If we take the limit  $\Delta z \rightarrow 0$  we obtain

$$\lim_{\Delta z \rightarrow 0} \left[ \langle |U(z+\Delta z) - U(z)|^2 \rangle \Delta z^{-2} \right] = \int_0^\infty d\beta \beta^2 E(\beta) \quad (5)$$

where the left side of the equality is the mean-square vertical shear  $S^2$ . Equation (5) demonstrates the relationship between the spectral density of a quantity and that of its gradient. In this case

$$\phi_s(\beta) = \beta^2 E(\beta) \quad (6)$$

where  $\phi_s(\beta)$  is the shear vertical wavenumber spectral density function. Relationship (6) is only applicable in the limit  $\Delta z \rightarrow 0$ . In general

$$\phi_s(\beta; \Delta z) = 4 \Delta z^{-2} E(\beta) \sin^2(\frac{1}{2}\beta \Delta z) \quad (7)$$

where  $\phi_s(\beta; \Delta z)$  is the spectral density of shear defined as the mean-square velocity differences over  $\Delta z$ , divided by  $\Delta z^2$ .

Gargett et al. (1980) have assembled a shear spectrum  $\phi_s(\beta)$  which we model as shown in Figure 1. The spectrum is flat to about 10 cpm where it takes a -1 slope to about 1 cpm. A high-wavenumber turbulence dissipation range exists beyond that point. We do not include contributions from that range in this analysis. We represent the spectrum as

$$\phi_s(\beta) = \phi_0 \quad , \quad \beta \leq \beta_* \quad ,$$

and

$$= \phi_0 \beta_*/\beta \quad , \quad \beta_c \leq \beta < \beta_* \quad , \quad (8)$$

$$= 0 \quad \beta_* < \beta \quad ,$$

where

$$\beta_* = 2\pi \times 10^{-1} \text{ rad m}^{-1} \quad (10 \text{ cpm})$$

and

$$\beta_c = 2\pi \text{ rad m}^{-1} \quad (1 \text{ cpm})$$

We substitute (6) and (8) into (4) and define to obtain

(9a)

where

$$I_1(y_*) = \int_0^{y_*} dy \quad y^{-2} \sin^2 y \quad , \quad (9b)$$

$$I_2(y_*, y_c) = \int_{y_*}^{y_c} dy \quad y^{-3} \sin^2 y \quad , \quad (9c)$$

and  $y_x = \frac{1}{2} B_x \Delta z$  and  $y_c = \frac{1}{2} B_c \Delta z$ . We integrate  $I_1$  and  $I_2$  to obtain

$$I_1(y_x) = \frac{1}{2} y_x^{-1} (\cos 2y_x - 1) + Si(2y_x), \quad (10a)$$

$$\begin{aligned} I_2(y_x, y_c) = & \frac{1}{4} [y_c^{-2} (\cos 2y_c - 1) - 2y_c^{-1} \sin 2y_c \\ & - y_x^{-2} (\cos 2y_x - 1) + 2y_x^{-1} \sin 2y_x] \\ & - Ci(2y_x) + Ci(2y_c), \end{aligned} \quad (10b)$$

where

$$Si(x) = \int_0^x dt t^{-1} \sin t \quad (10c)$$

and

$$Ci(x) = - \int_x^\infty dt t^{-1} \cos t \quad (10d)$$

are the sine and cosine integrals which are available in tabular form.

### 3.0 RESULTS

Given a value of  $\Delta z$ , equations (9) and (10) yield an estimate of the mean-square velocity difference as a function of the spectral amplitude  $\phi_0$ . We have computed a number of estimates of  $\frac{1}{2} \phi_0^{-1} \langle |A\dot{u}|^2 \rangle$  which are shown in Table 1, and are plotted in Figure 2. A linear trend is evident for  $\Delta z$  greater than about 5m. The mean-square velocity difference over 16m is about 12 times the differences over 2m; the root-mean-square difference over 16m (which might be used to characterize the distortion rate) is about 3.5 times the values over 2m. Table 1 also shows

**Table 1** Mean-square velocity differences versus spacing  $\Delta z$ . Entry with subscript  $\beta L \tilde{\beta}$  refers to mean-square difference due to contributions of components with wavelengths larger than  $2\Delta z$ .  $r$  is the ratio of this mean-square difference to the mean-square difference with all wavenumbers contributing.

$\Delta z(m)$	$\frac{1}{2} \phi_0^{-1} \langle  \Delta u ^2 \rangle$	$\frac{1}{2} (\phi_0 \Delta z)^{-1} \langle  \Delta u ^2 \rangle$	$\frac{1}{2} (\phi_0 \Delta z)^{-1} \langle  \Delta u ^2 \rangle_{\beta L \tilde{\beta}}$	$r$
2	2.14	1.072	1.00	0.93
4	5.47	1.367	1.20	0.88
5	7.10	1.419	1.22	0.86
8	11.78	1.473	1.22	0.83
10	14.90	1.490	1.22	0.82
16	24.24	1.515	1.22	0.80

$\frac{1}{2}(\phi \Delta z)^{-1} \langle |\Delta u|^2 \rangle$  which clearly approaches an asymptotic value of about 1.52. Note that  $\langle |\Delta u|^2 \rangle \propto \Delta z$  for large  $\Delta z$ . This implies that  $S^2(\Delta z) \propto \Delta z^{-1}$ : we observe this sort of behavior in the YVETTE shear estimates.

In order to characterize the contribution of components with vertical wavenumbers less than any given value  $\tilde{\beta}$  to the mean-square velocity difference, (which we will denote as  $\langle |\Delta u|^2 \rangle_{\beta < \tilde{\beta}}$ , we simply repeat the above analysis but with the upper limit of integration in (4) set to  $\tilde{\beta}$ . Of special interest might be the contribution to the mean-square velocity difference over  $\Delta z$  due to components with vertical scales greater than  $\Delta z$ . We define  $\tilde{\beta} = \pi/\Delta z$  which means that we are considering the contributions to the mean-square velocity difference of components with wavelengths  $2\pi\tilde{\beta}^{-1} = 2\Delta z$  and longer.

The results of these calculations are also shown in the table (column 4). The value of  $\frac{1}{2}(\phi \Delta z)^{-1} \langle |\Delta u|^2 \rangle_{\beta < \tilde{\beta}}$  approaches an asymptotic value of 1.22. Also shown in the table is the ratio

$$r = \langle |\Delta u|^2 \rangle_{\beta < \tilde{\beta}} / \langle \mu u \rangle^2$$

The results show that 93% of the mean-square velocity difference over 2m is due to components with wavelengths of 4m and longer. This value drops to asymptotically about 80%.

#### 4.0 DISCUSSION AND A SIMPLE SIMULATION

These results, which are based on a spectral-density-function model, suggest that the mean-square velocity difference over values of  $\Delta z$  in our range of interest increase roughly as  $\Delta z$  and that  $S^2(\Delta z) \equiv \langle (\Delta u)^2 \rangle \Delta z^{-2}$  behaves as  $\Delta z^{-1}$ . Trends of this sort are evident in YVETTE data. If we characterize the relative distortion rate between locations  $\Delta z$  apart as  $\langle |\Delta u|^2 \rangle^{1/2}$ , we see that the distortion rate behaves as  $\Delta z^{1/2}$ . This implies that the treatment of velocity variation as a linear variation over scales of interest, for wake model application say, may be inappropriate. However, 90% or better of the root-mean-square distortion rate of two points separated by  $\Delta z$  is given by components with wavelengths  $2\Delta z$  and longer. This means that while we can adequately characterize the distortion rate between two points separated by  $\Delta z$  with velocity data resolved to wavelengths of  $2\Delta z$  and longer, we should not characterize the distortion between these locations with a linear variation.

In an attempt to make these results more vivid, we undertook an elementary kinematic "wake" simulation using the velocity field recorded during YVETTE deployment 09 in the Western Sargasso (Lambert et al., 1980). The velocity profile is shown in Figure 3; the data have an effective resolution of about 3m. We computed the distortion of initially nearly circular (10m diameter) patterns of passive tracers located in depth intervals 70-80m, 110-120m, 220-230m, 345-355m, with the velocity field fixed over the simulation time interval. The resulting "wake" cross-sections to one-hour time-late are shown in Figure 4.

In three of the four cases, there clearly is substantial distortion over scales less than the initial wake cross section.

Finally, we note that the work of Patterson et al. (1981) with YVETTE data suggests that  $\overline{S^2}(\Delta t=2m) \approx \overline{N^2}$ , where  $\overline{N^2}$  is the mean (depth averaged) Brunt-Väisälä frequency. If the spectral shear representation is appropriate we can estimate  $S^2$  over other  $\Delta t$  via (9) and the estimate of  $\phi_0$  given  $S^2(\Delta t=2m)$ .

SHEAR SPECTRAL MODEL AND CORRESPONDING  
MEAN-SQUARE VELOCITY DIFFERENCE OVER  $\Delta z$

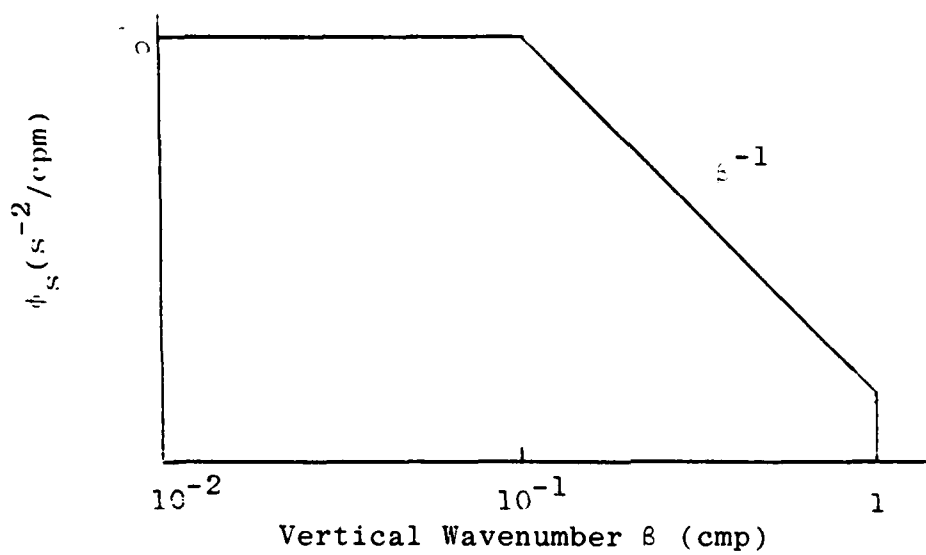


Figure 1 Shear Spectral Model After Gargett et al. (1980)

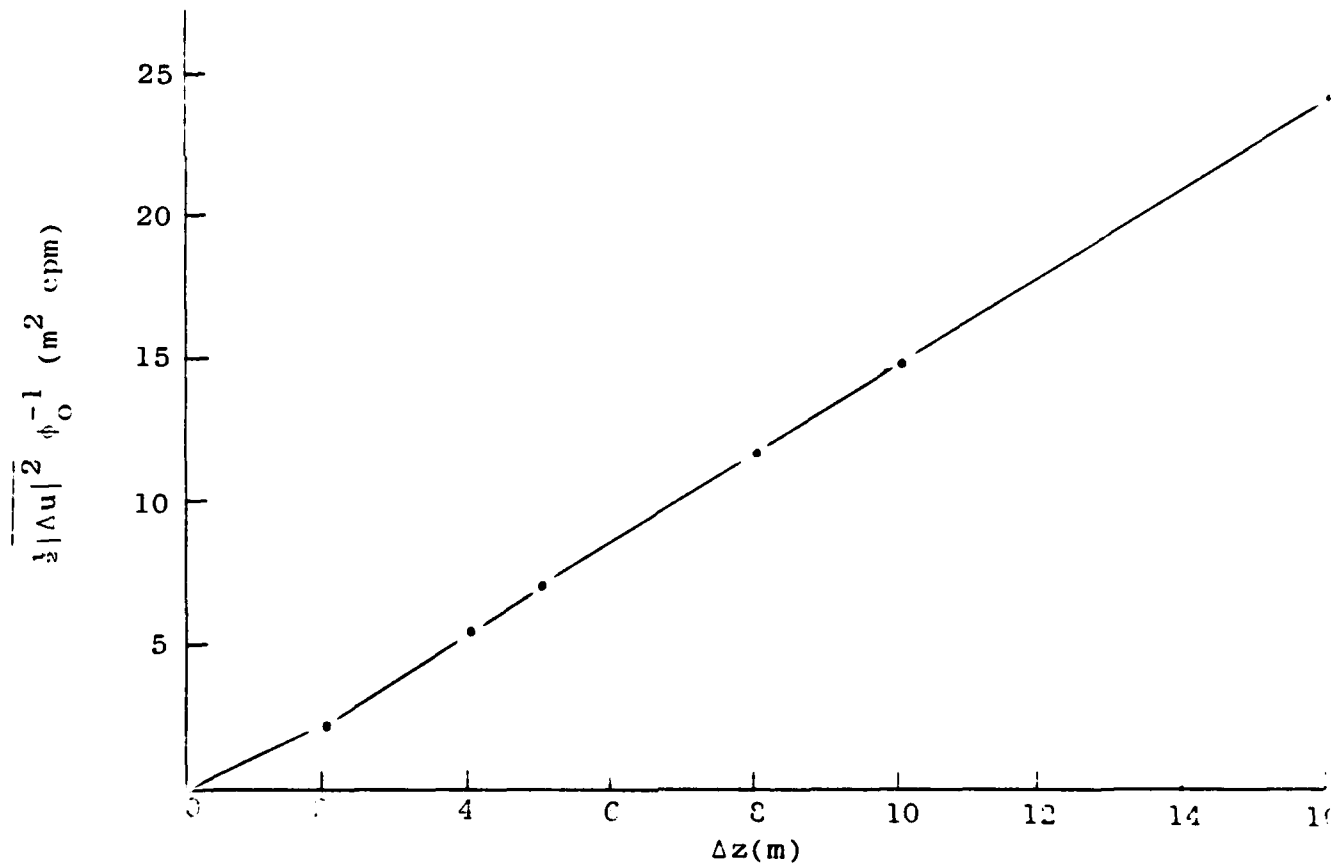


Figure 2 Mean-Square Velocity Difference Over  $\Delta z$ .

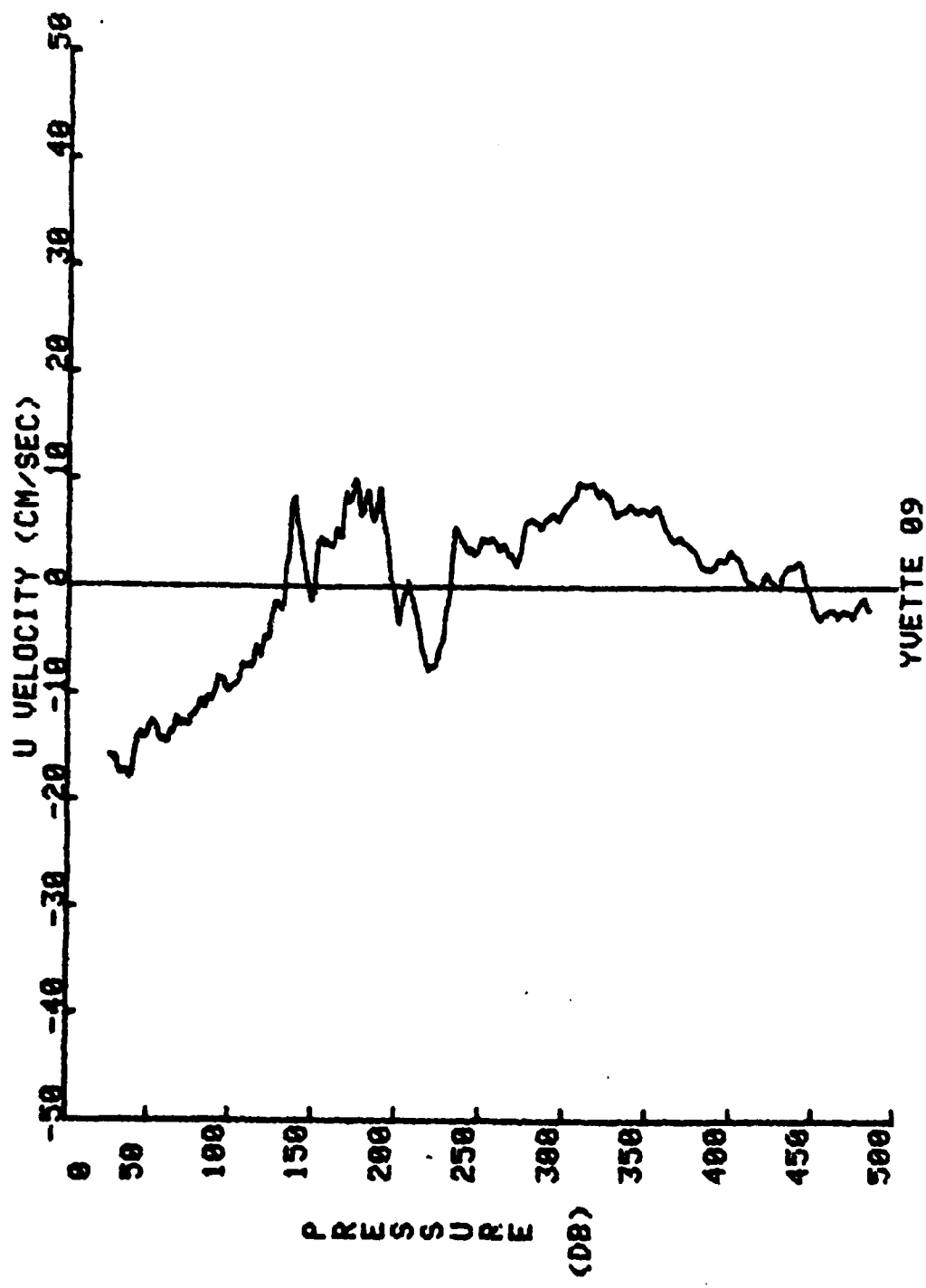
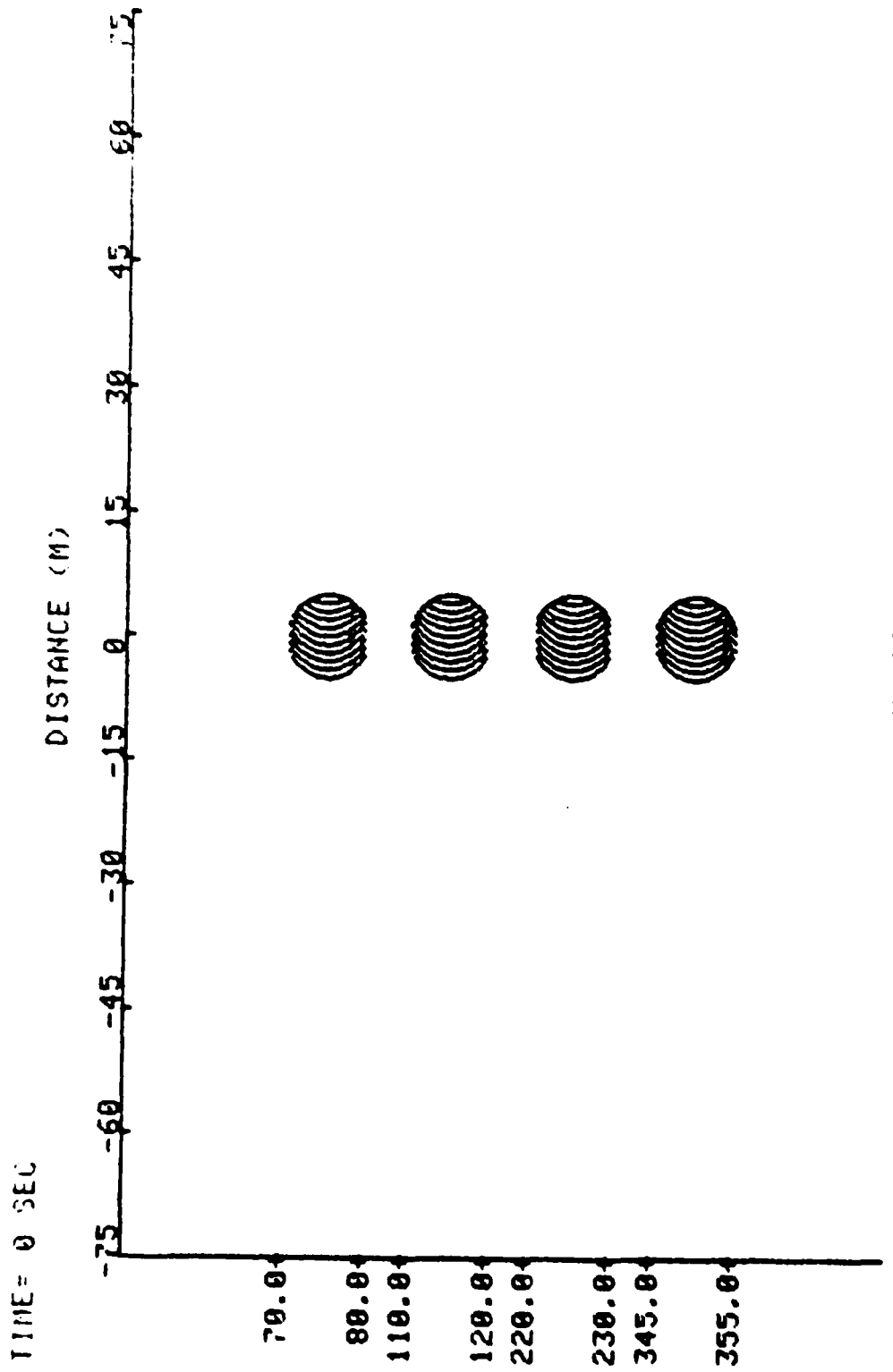


Figure 3 YVETTE 09 Velocity Profile used for Simulations



YVETTE 09

Figure 4 Distortion of nearly circular pattern of passive tracers in YVETTE 09 velocity field. Note the discontinuous vertical scale.  
 (a) Initial Pattern

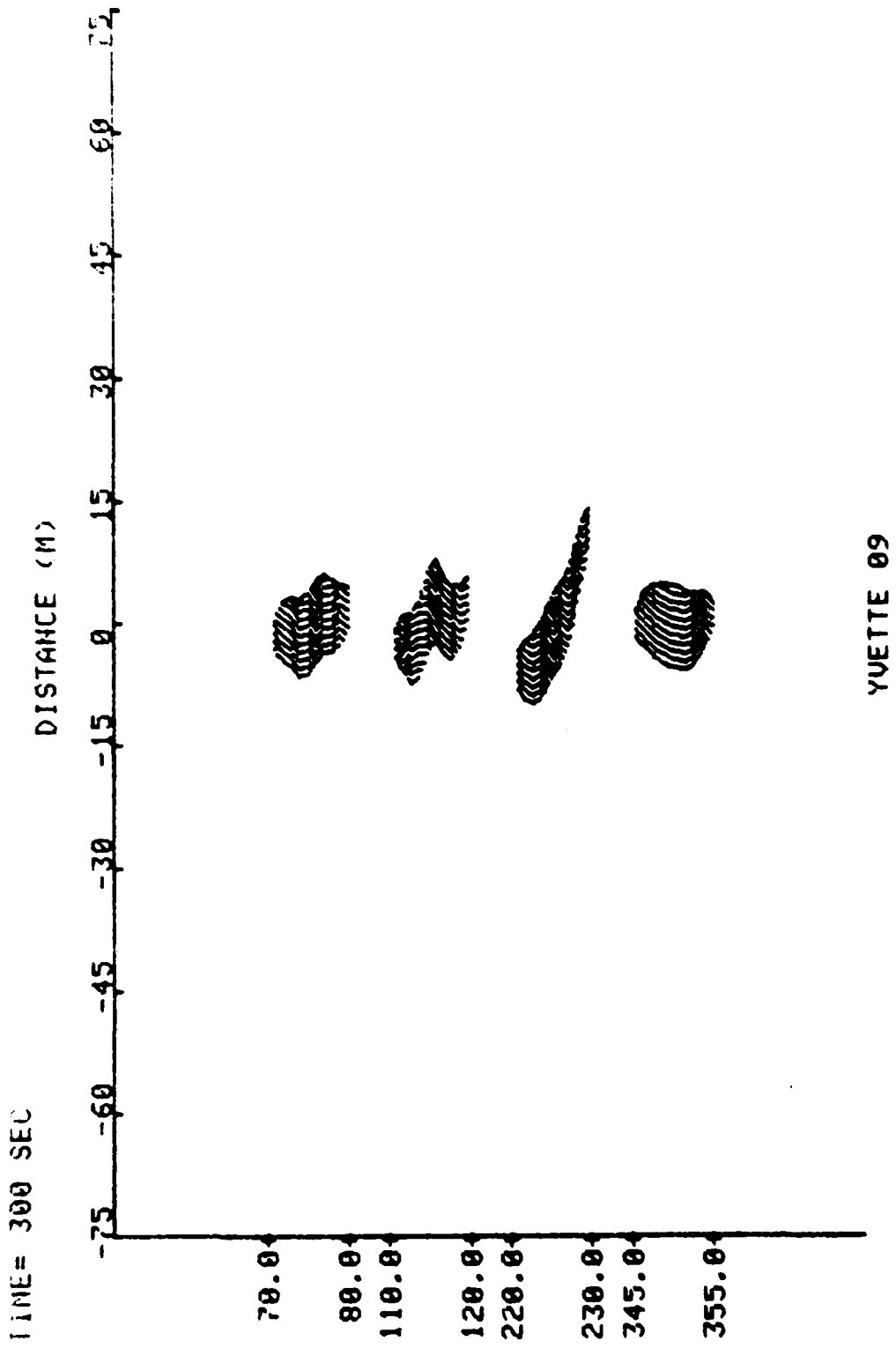
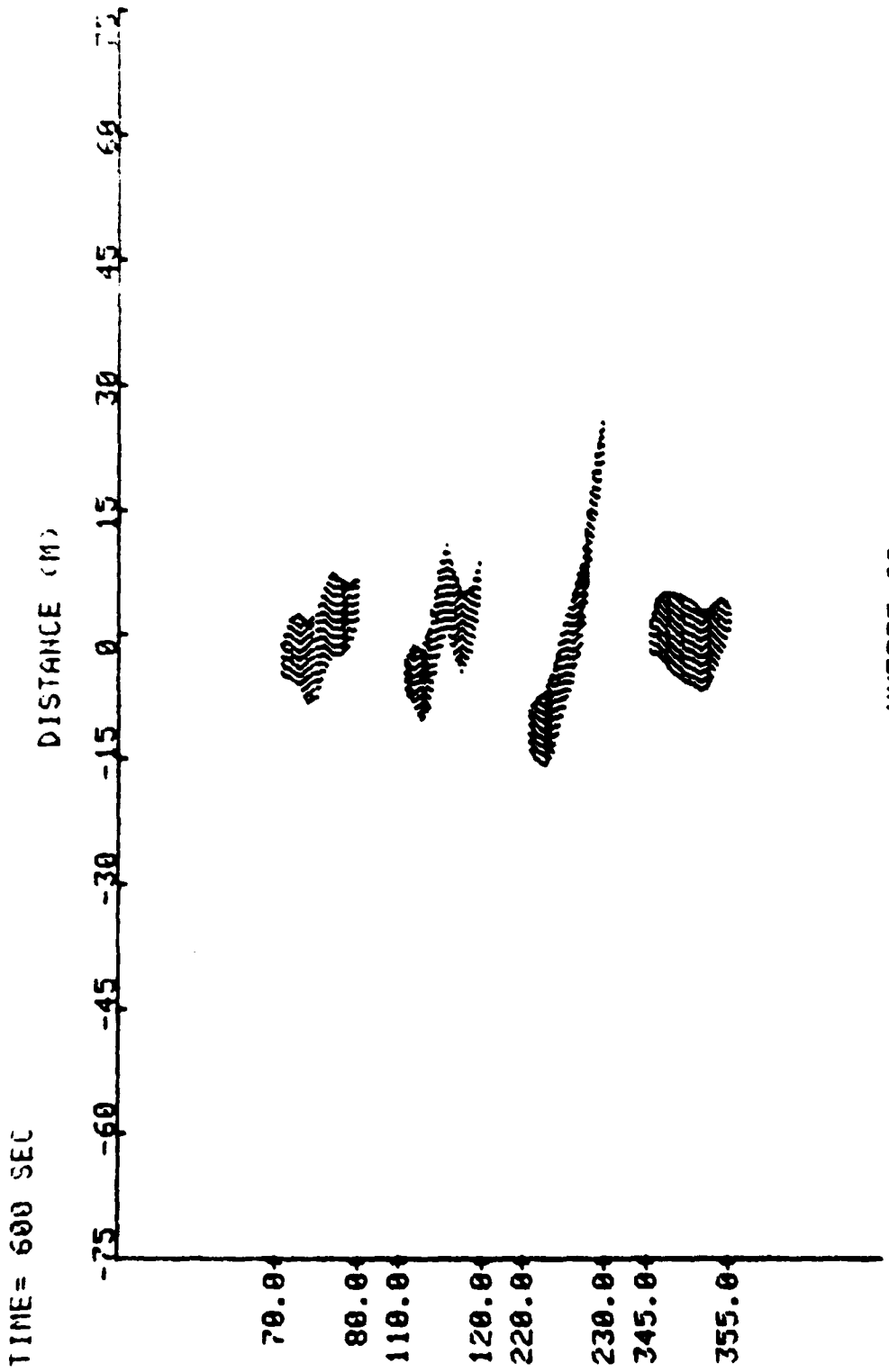


Figure 4(b) Pattern after 5 minutes



YUETTE 09

Figure 4(c) Pattern after 10 minutes

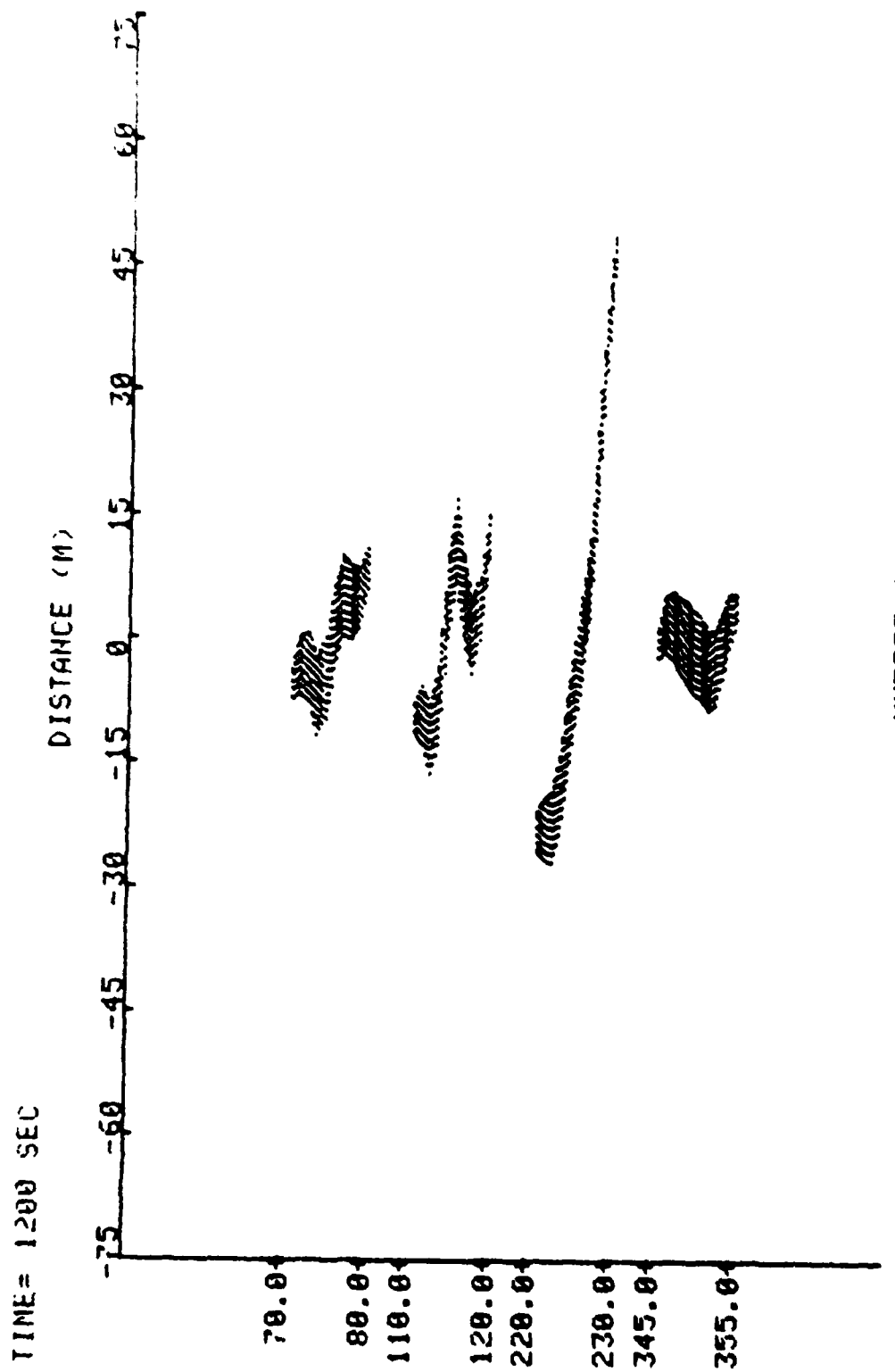


Figure 4(d) Pattern after 20 minutes



Figure 4(e) Pattern after 40 minutes

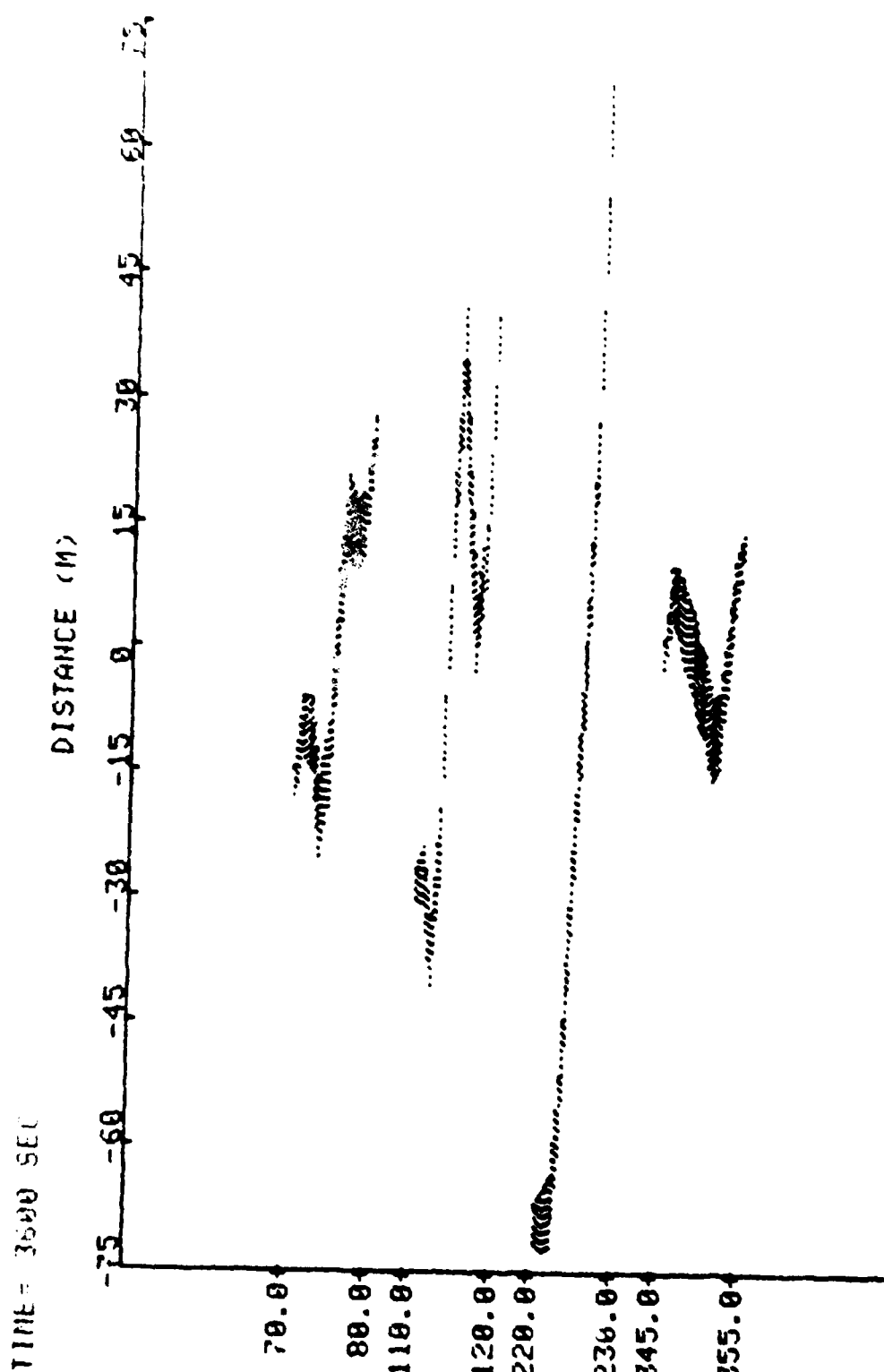


Figure 4(f) Pattern after 60 minutes

## REFERENCES

- Gargett, A. E., P. J. Hendricks, T. B. Sanford, T. R. Osborn, and A. J. Williams III (1980): A composite spectrum of vertical shear in the upper ocean from the profilers EMVP, SCIMP and CAMEL, Pacific Marine Science Report 80-11, Institute of Ocean Science, Sidney, B. C.
- Lambert, R. B., Jr., D. L. Evans and P. J. Hendricks, 1980: Data Report-SCIMP and YVETTE, Progres Report I, Ocean Physics Div. Tech Rept. 80-201-04, Science Applications, Inc., McLean, VA.
- Patterson, S. L., F. C. Newman, D. M. Rubenstein and R. B. Lambert, Jr. (1981): Spatial distribution of vertical shear, SAI Technical Report 81-201-02, Science Applications, Inc.

NORDA DISTRIBUTION LIST FOR  
REPORT NO. SAI-82-485-WA  
ENTITLED "SPECTRAL MODEL PREDICTIONS OF  
MEAN-SQUARE-SHEAR DISTORTION RATES"

Naval Ocean Research and  
Development Activity  
Code 100, 110, 300, 320,  
330, 340, 350, 360  
(one copy each)  
NSTL Station, MI 39529

Naval Ocean Research and  
Development Activity  
Code 540  
NSTL Station, MI 39529 (5)

NORDA Liaison Office  
800 N. Quincy St., Rm. 502  
Arlington, VA 22217 (1)

Office of Naval Research  
Code 102C  
800 North Quincy Street  
Arlington, VA 22217  
ATTN: Dr. R. Winokur (1)

Office of Naval Research  
Code 103T  
800 North Quincy Street  
Arlington, VA 22217  
ATTN: Dr. S. G. Reid (1)

Office of Naval Research  
Code 480  
800 North Quincy Street  
Arlington, VA 22217  
ATTN: Dr. L. Goodman (1)

Commander  
Naval Oceanography Command  
NSTL Station, MS 39529 (1)

Dr. A. Andreassen  
OP-95T  
Pentagon  
Washington, D.C. 20350 (1)

Chief of Naval Operations  
Department of the Navy  
OP-952  
Washington, D.C. 20350  
ATTN: CDR Harlett (2)

CAPT H. E. Marxer  
OP-212E  
Pentagon  
Washington, D.C. 20350 (1)

Commanding Officer  
Naval Research Laboratory  
Washington, D.C. 20375 (1)

Naval Research Laboratory  
Code 4340  
Washington, D.C. 20375 (1)

Commanding Officer  
Naval Oceanographic Office  
NSTL Station, MS 39529 (1)

Naval Oceanographic Office  
Code 7004  
NSTL Station, MS 39529 (1)

Naval Oceanographic Office  
Code 7200  
NSTL Station, MS 39529 (1)

Commanding Officer  
Naval Ocean Systems Center  
San Diego, CA 92152 (1)

Naval Electronics Systems Command  
Code 320  
Washington, D.C. 20360 (1)

Naval Electronics Systems Command  
PME 124  
Washington, D.C. 20360 (1)

Dr. W. Welch  
TRIDENT Systems Project Office  
National Center 3  
Room 7W66  
Washington, D.C. 20360 (1)

Dr. G. D. Smith  
Applied Physics Laboratory  
The Johns Hopkins University  
Johns Hopkins Road  
Laurel, MD 20810 (1)

Dr. L. J. Smith  
Applied Physics Laboratory  
The Johns Hopkins University  
Johns Hopkins Road  
Laurel, MD 20810 (1)

Dr. G. E. Merritt  
Applied Physics Laboratory  
The Johns Hopkins University  
Johns Hopkins Road  
Laurel, MD 20810 (1)

Dr. H. E. Gilreath  
Applied Physics Laboratory  
The Johns Hopkins University  
Johns Hopkins Road  
Laurel, MD 20810 (1)

Dr. R. Hoglund  
Office, Assistant Sec. of Navy  
Pentagon  
Room 4-D745  
Washington, D.C. 20350 (1)

Dr. P. A. Selwyn  
Strategic Support Projects Office  
SP-2023  
Department of the Navy  
Washington, D.C. 20376 (1)

Dr. Melbourne G. Briscoe  
Woods Hole Oceanographic Inst.  
Woods Hole, MA 02543

Dr. T. Sanford  
University of Washington  
Applied Physics Laboratory  
1013 NE Fortieth Street  
Seattle, WA 98195 (1)

Naval Intelligence Support Center  
Code 600  
4301 Suitland Road  
Washington, D.C. 20390 (1)

Naval Underwater Systems Center  
New London Laboratory  
Code 60  
New London, CT 06320 (1)

Administrative Contracting Officer  
Defense Contract Administration  
Services  
Management Area - San Diego  
Code S0514A  
Bldg. 4, AF Plant 19, 4297  
Pacific Hwy.  
San Diego, CA 92110 (1)

Director  
Naval Research Laboratory  
Code 2627  
Washington, D.C. 20375 (6)

Defense Technical Information  
Center  
Code S47031  
Bldg. 5, Cameron Station  
Alexandria, VA 22314 (12)

Office of Naval Research  
Code N62887  
Western Regional Office  
1030 E. Green Street  
Pasadena, CA 91106 (1)

**FILMED**

